Supplementary

A Method for a Column-by-Column EELS Quantification of Barium Lanthanum Ferrate

Judith Lammer[a,*], Christian Berger[b], Stefan Löffler[c], Daniel Knez[a], Paolo Longo[d], Gerald Kothleitner[a], Ferdinand Hofer[a], Georg Haberfehlner[a], Edith Bucher[b], Werner Sitte[b], Werner Grogger[a]

(a) Institute of Electron Microscopy and Nanoanalysis (FELMI), Graz University of Technology & Graz Centre for Electron Microscopy (ZFE), Steyrergasse 17, 8010 Graz, Austria

(b) Chair of Physical Chemistry, Montanuniversitaet Leoben, Franz-Josef-Straße 18, 8700 Leoben, Austria

(c) University Service Centre for Transmission Electron Microscopy (USTEM), TU Wien, Wiedner Hauptstraße 8-10, 1040 Vienna, Austria

(d) Gatan Inc., 5794 W Las Positas Blvd, Pleasanton, CA 94588, USA

*corresponding author: judith.lammer@tugraz.at (J. Lammer)

The first chapter gives further information on the crystal structure of $Ba_{1.1}La_{1.9}Fe_2O$. The subsequent two chapters of this supplement cover the theoretical considerations, which lead to the equations used in the main paper. The last chapter describes the synthesis of the material.

Crystal structure of $Ba_{1.1}La_{1.9}Fe_2O$

The layers of the Ruddlesden-Popper phase are described as two different crystal types, which are stacked together: the first is structured like a perovskite, while the second follows the NaCl structure (rock salt layer). As shown in Fig. S.1, the two layers are overlapping in [100] direction. Therefore, it is easier to differentiate between them when displaying the octahedra for the B-sites (Fe):

- regions within the connected octahedra belong to the perovskite layer (including the A-sites which are trapped by the octrahedra)
- regions outside the connected octahedra belong to the rock salt layer

Two perovskite layers separated by a rock salt layer are offset by half the size of a unit cell in b-direction.

The edges of the unit cell (as used in this manuscript) do not coincide with the edges of the layers. The unit cell (from left to right) starts with half of a perovskite layer, next to a rock salt layer, next to a whole perovskite layer, next to another rock salt layer and finally again half of a perovskite layer.

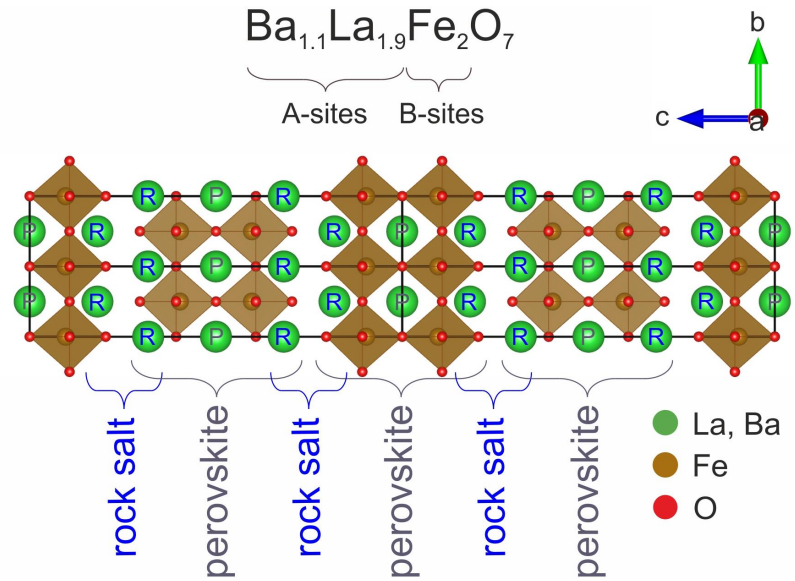

Fig. S.1: Four unit cells (marked with black rectangles) in [100] direction. A-sites in the perovskite layer are marked with the letter “P” and in the rock salt layer with the letter “R”.

Assumptions for the off-axis signal correction

We assume the following:

The A-sites only contain Ba and La atoms. We only considered the EELS signal from the A-sites. The simulations described in the paper show that the relative additional intensity from neighbouring Ba/La columns does not depend much on the individual composition of these columns but rather stays constant over the whole unit cell. Therefore, we calculated mean off-axis contributions from the simulations and performed the following corrections for the Ba and La intensities:

$$\mathrm{I_{Ba}} = \mathrm{I_{Ba}^{exp}} - 0{,}183 \cdot \mathrm{I_{\varnothing Ba}} \qquad \text{A.1}$$

$$\mathrm{I_{La}} = \mathrm{I_{La}^{exp}} - 0{,}188 \cdot \mathrm{I_{\varnothing La}} \qquad \text{A.2}$$

with:

I_x: net intensity of ionization edge

I_x^{exp}: experimentally determined intensity of ionization edge (including off-axis signal)

$I_{\varnothing x}$: mean off-axis intensity of the ionization edge over the unit cell

EELS quantification

A conventional (absolute) EELS quantification neglecting channelling effects follows the well-known scheme and yields the number of atoms per unit area [1]:

$$\mathrm{n_{Ba}} = \frac{\mathrm{I_{Ba}}}{\mathrm{I_0}\ \sigma_{\mathrm{Ba}}} \qquad \text{A.3}$$

$$\mathrm{n_{La}} = \frac{\mathrm{I_{La}}}{\mathrm{I_0}\ \sigma_{\mathrm{La}}} \qquad \text{A.4}$$

with:

I_x: net intensity of ionization edge

I_0: incident intensity

σ_x: ionization cross section

n_x: number of atoms per unit area

From the number of atoms, the concentration values (atomic percent) can be calculated:

$$c_{La} = \frac{n_{La}}{n_{La} + n_{Ba}} = \frac{I_{La}}{(n_{La} + n_{Ba})\, I_0\, \sigma_{La}} \quad \text{A.5}$$

$$c_{Ba} = \frac{n_{Ba}}{n_{La} + n_{Ba}} = \frac{I_{Ba}}{(n_{La} + n_{Ba})\, I_0\, \sigma_{Ba}} \quad \text{A.6}$$

Introducing a proportionality factor α_x, the relationship between I_x and c_x can be simplified:

$$I_{Ba} = c_{Ba}\, \alpha_{Ba} \quad \text{A.7}$$

$$I_{La} = c_{La}\, \alpha_{La} \quad \text{A.8}$$

with:

$\alpha_x = (n_{Ba} + n_{La})\, I_0\, \sigma_x$

$n_{Ba} + n_{La}$: total number of atoms/ions in one A-site column

Considering that the concentrations need to add up to 100%, we can express the La intensity by the Ba intensity and vice versa:

$$c_{Ba} + c_{La} = \frac{I_{Ba}}{\alpha_{Ba}} + \frac{I_{La}}{\alpha_{La}} = 1 \quad \text{A.9}$$

$$I_{Ba} = -\frac{\alpha_{Ba}}{\alpha_{La}} \cdot I_{La} + \alpha_{Ba} \quad \text{A.10}$$

$$I_{La} = -\frac{\alpha_{La}}{\alpha_{Ba}} \cdot I_{Ba} + \alpha_{La} \quad \text{A.11}$$

The linear relationship in equations A.10 and A.11 allows us to plot measured (corrected) intensities from atomic columns with different amounts of Ba and La as a scatter plot (see Fig. 4 in the paper). Then we perform a linear regression and determine the slope and the intercept of the resulting straight line. For the fitting algorithm, one has to be careful that the Ba and La signals have uncertainties, which do not depend on each other and that Ba may be plotted over La and vice versa. Therefore an appropriate least square fitting algorithm must be chosen (York method [2,3]). From *k* and *d* we can then compute the factors α_{Ba} and α_{La}:

$$I_{La} = I_{Ba} \cdot k + d \quad \text{A.12}$$

$$k = -\frac{\alpha_{La}}{\alpha_{Ba}} \quad \text{A.13}$$

$$d = \alpha_{La} \quad \text{A.14}$$

$$\alpha_{Ba} = -\frac{d}{k} \quad \text{A.15}$$

Equations A.14 and A.15 reveal that the factors α_{Ba} and α_{La} correspond directly to the x- and y- intercepts of the straight line. Once we know the values for α_x we basically know the total number of atoms in the atomic column and can now get access to the concentrations for each atomic column:

$$c_{Ba} = \frac{I_{Ba}}{\alpha_{Ba}} \quad \text{A.16}$$

$$c_{La} = \frac{I_{La}}{\alpha_{La}} \quad \text{A.17}$$

Synthesis of the material

$Ba_{1.1}La_{1.9}Fe_2O$ was synthesised via a citric acid – ethylenediaminetetraacetate (EDTA) sol-gel method, by mixing stoichiometric amounts of the metal nitrates ($La(NO_3)_3 \cdot 6H_2O$, $Ba(NO_3)_2$, and $Fe(NO_3)_3 \cdot 9H_2O$; all chemicals obtained from Sigma Aldrich, analytical grade quality) with distilled H_2O in a stainless steel vessel. After the metal nitrates were completely dissolved, anhydrous citric acid and EDTA (one mole each per mole cation) were added. Subsequently, 25% aqueous NH_3 solution was used to obtain pH = 8 and a clear dark blue solution. The temperature was slowly raised to remove water and form a gel until self-ignition of the gel occurred.

The raw ash was crushed in an agate mortar and calcined at 1350 °C for 4 h (5 K/min ramps for heating and cooling) in air. The calcined powder was single phase according to XRD and showed a broad particle size distribution of d_{50} = 20 – 30 µm (measured with laser scattering using a CILAS 1064L particle size analyser). A bench top roll-mill was used to grind the calcined powder with ZrO_2 balls (3 mm diameter) in ethanol for 72 h until a final average particle size of d_{50} = 0.8 µm was obtained. The calcined powder was isostatically pressed at

250 MPa and sintered at 1350 °C for 4 h (heating and cooling rates of 5 K/min), to obtain a cylindrical sample (5.72 mm length x 9.12 mm diameter). The relative density of the pellet was 86% (determined via the geometrical method) of the theoretical density as obtained by X-ray diffraction (ρ_{XRD} = 6.594 g cm^{-3}).

References

[1] R.F. Egerton, Electron Energy-Loss Spectroscopy in the Electron Microscope, Springer US, Boston, MA, 2011.

[2] D. York, N.M. Evensen, M.L. Martínez, J. de Basabe Delgado, Unified equations for the slope, intercept, and standard errors of the best straight line, American Journal of Physics 72 (2004) 367–375. https://doi.org/10.1119/1.1632486.

[3] D. York, LEAST-SQUARES FITTING OF A STRAIGHT LINE, Can. J. Phys. 44 (1966) 1079–1086. https://doi.org/10.1139/P66-090.